Effect of the Ionic Concentration of Simulated Body Fluid on the Minerals Formed on Crosslinked Elastin-Like Polypeptide Membranes

Ophélie Gourgas[1], Gregory B. Cole[2,3], Lisa D. Muiznieks[2], Simon Sharpe[2,3], Marta Cerruti[1*].

[1] Department of Mining and Materials Engineering, McGill University, Montreal, Canada;

[2] Molecular Medicine, Hospital for Sick Children, Toronto, ON, Canada;

[3] Department of Biochemistry, University of Toronto, Toronto, ON, Canada;

* Corresponding author at: Materials Engineering, McGill University, 3610 University St., 2M020 Wong Building, Montreal, Quebec H3A 0C5, Canada. E-mail address: marta.cerruti@mcgill.ca (M. Cerruti). Phone number: 514 398 5496.

SUPPLEMENTAL MATERIAL

This document contains supplemental material related to:

- **Section 1**: Detailed methods
- **Section 2**: Supplemental figures and tables
- **Section 3**: Supplemental references

Section 1: Detailed methods

Determination of the apatite ionic activity products (IP) and degree of supersaturation (S)

An increase in concentration of calcium (Ca) and phosphate (P) ions in the simulated body fluid (SBF) leads to an increase in the apatite ionic activity product (IP) of the SBF.

Formation of hydroxyapatite (HA) from its constituent ions is given by the following equilibrium (1):

$$Ca_{10}(PO_4)_6(OH)_2 \Leftrightarrow 10Ca^{2+} + 6PO_4^{3-} + 2OH^-, \text{ (i)}$$

The ionic activity product (IP) of HA in an aqueous solution is this given by the following equation (1):

$$IP = (\gamma_{Ca^{2+}})^{10} (\gamma_{PO4^{3-}})^{10} (\gamma_{OH^-})^2 [Ca^{2+}]^{10} [PO_4^{3-}]^6 [OH^-]^2, \text{ (ii)}$$

where γ is the activity coefficient, and [ ] represents ionic concentration.

The activity coefficients were calculated based on the modified Debye-Hückel equation proposed by Davies (2). The IP of each SBF solution is given in Table S1.

The relative degree of supersaturation S with respect to apatite phases was calculating using the following equation (1):

$$S = (IP/K_{sp})^{1/n}, \text{ (iii)}$$

where IP is the ionic activity, K_{sp} the solubility product, and n the number of ions in a formula unit (i.e. 18 for apatite). K_{sp} of apatite in water is 5.5×10^{-118} at 37 °C (3).

The degree of supersaturation S of each SBF solution in respect to apatite is given in Table S1.

Determination of the crystallinity index (CI) of the minerals by FTIR

The splitting of the v_4 PO_4^{3-} band can be used to estimate HA crystallinity index (CI) according to the formula introduced by Shemesh *et al*. (4):

$$CI = (A602 + A562) / A588, \text{ (iv)}$$

where A_X is the absorbance at wavenumber x (Figure S7)

A higher degree of splitting and therefore a higher CI correspond to more crystalline materials (5).

Ca K-edge Near Edge X-ray absorption fine structure (Ca K-edge NEXAFS) spectroscopy

- **Spectra acquisition**

We used NEXAFS spectroscopy to identify and quantify the Ca-P phases present in the samples. NEXAFS is a synchrotron-based technique that allows analyzing how x-rays are absorbed by an atom at energies near the core-level binding energies of that atom depending on its chemical and physical environment (6). Because of crystallinity is not required for NEXAFS measurements, this technique is well suited for analysis of non-crystalline or poorly crystalline phases (6). Also, NEXAFS is more sensitive than traditional spectroscopic techniques, with a detection limit that can be as low as few ppm. Thus, NEXAFS is an excellent tool to analyze et differentiate the Ca-P phases present in calcified ELP_3 membranes.

Ca K-edge spectra were collected in fluorescence mode with energies between 1.7 and 10 keV and with a photon beam spot size of 2 mm x 6 mm. The storage ring energy during data collection was 2.9 GeV ant the current around 200 mA. The X-ray beam was monochromated by Si (111) crystals with energy resolution ($\Delta E/E$) of 10^{-4}.

- **Data analysis**

We first selected seven reference compounds (Figure S6). The first one is ELP_3 membranes incubated in 3.8 mM $CaCl_2$ for 16 days (ELP_3-Ca^{2+}). This serves as a model of Ca ions adsorbed on ELP_3. The other five references are Ca species that are known to be present in pathological calcifications: amorphous calcium phosphate (ACP), octacalcium phosphate (OCP), dicalcium phosphate dihydrate (DCPD), hydroxyapatite (HA), carbonated hydroxyapatite (CHA), and β-tricalcium phosphate (β-TCMP) (7-13).

To determine and quantify the Ca-P phases in the ELP_3 samples, we performed linear combination fitting (LCF) analysis using Athena software (Demeter 0.9.20). LCF is justified because the x-ray absorption from different species in a sample is additive (14). The total absorption coefficient calculated by LCF can be written as:

$$M = \Sigma_i f_i (STD_i), (v)$$

where M is the least square fit to the sample spectrum, (STD_i) represents the absorption coefficient of the standard reference spectra, and f_i is the fraction of each reference spectrum in the sample spectrum, summed over the number of references, i. Thus, with appropriate standard references, LCF can identify and quantify the fraction of chemical species in an unknown sample (14).

We first performed principal component analysis (PCA) to determine which reference compounds should be excluded for the LCF fitting and thus avoid using an excessive number of standard compounds. PCA results showed that DCPD and β-TCMP were not likely present in the calcified membranes. Thus, we used ELP_3-Ca^{2+}, ACP, OCP, HA, and CHA as references for the LCF analysis. We performed LCF using all the possible combinations of the selected reference compounds. We evaluated the quality of the fits using the R-factor: fitting results with R-factor values below 0.02 are considered satisfactory (15). We reported the LCF combination giving the lowest R-factor for each sample analyzed (Table S16).

Section 2: Supplemental figures and tables

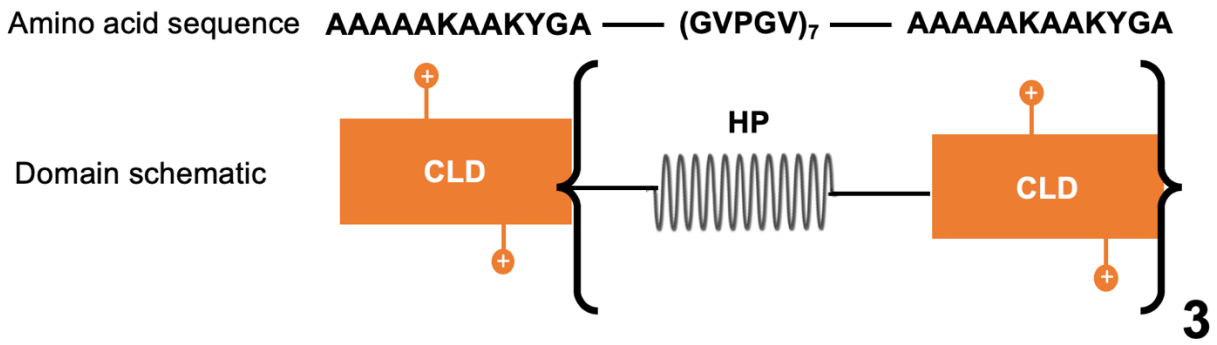

Figure S1. The repeating amino acid sequence and alternating domain architecture of ELP_3. Crosslinking domains (CLD) and hydrophobic domains (HP) are represented as orange rectangles and springs, respectively.

Table S1. Ion concentrations, apatite ionic activity products (IP), and degree of supersaturation (S) of human blood plasma, 1 x, 1.5 x, 2 x, and 3 x simulated body fluid (SBF) solutions.

	Ion concentration (mM)									
Solution	Na^+	K^+	Mg^{2+}	Ca^{2+}	Cl^-	HCO_3^-	HPO_4^{2-}	SO_4^{2-}	Log IP	S
Blood plasma	142.0	5.0	1.5	2.5	103.0	27.0	1.0	0.5	-96.6	14
1 x SBF	142.0	5.0	1.5	2.5	147.8	4.2	1.0	0.5	-96.6	14
1.5 x SBF	211.5	7.5	2.4	3.8	228.0	6.3	1.5	0.8	-93.8	20
2 x SBF	282.0	10.0	3.0	5.0	304.0	8.4	2.0	1.0	-91.9	26
3 x SBF	423.0	15.0	4.8	7.6	456.0	12.6	3.0	1.6	-87.5	45

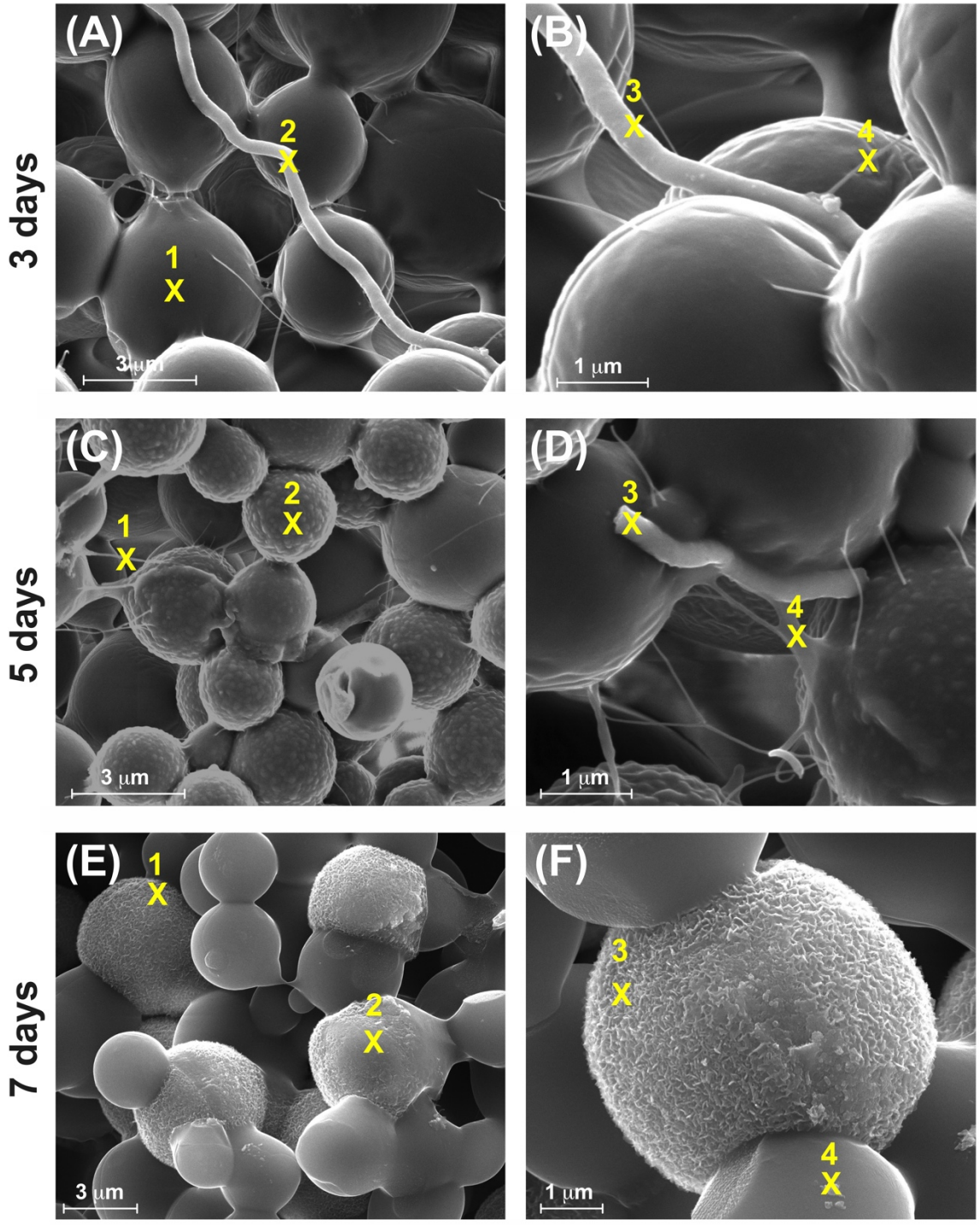

Figure S2. SEM images of ELP_3 membranes after incubation in 1.5 x SBF for (**A** and **B**) 3, (**C** and **D**) 5, and (**E** and **F**) 7 days. The spots marked with "X" on all panels indicate the spots where EDS spectra were collected and they correspond to the data presented in Tables S2 (spots in **A, B**), S4 (spots in **C, D**), and S5 (spots in **E, F**).

Table S2. Relative elemental atomic percentages measured by EDS in ELP_3 membranes incubated in 1.5 x SBF for 3 days. The spots 1-4 are shown in Figures S2A and S2B.

Spot	C (at%)	O (at%)	N (at%)	Ca (at%)	P (at%)	O/C	N/C	Ca/P	N/Ca
1	67.2	17.8	15.0	0	0	0.26	0.22	/	/
2	64.8	21.6	12.9	0.4	0.3	0.33	0.20	1.3	32.3
3	64.4	26.3	7.4	1.3	0.9	0.41	0.11	1.4	5.7
4	68.1	20.8	10.4	0.6	0.1	0.31	0.15	6.0	17.3

Table S3. List of Ca-P compounds found in pathological calcifications and their Ca/P atomic ratios (16).

Name	Formula	Ca/P ratio
Amorphous calcium phosphate (ACP)	$Ca_3(PO_4)_2.3H_2O$	1.5
Octacalcium phosphate (OCP)	$Ca_8H_2(PO_4)_6.\ 5H_2O$	1.33
Dicalcium phosphate dihydrate (DCPD)	$Ca(HPO_4).2H_2O$	1.0
Magnesium- substituted β-tricalcium phosphate (β-TCMP)	$Ca_{18}(Mg)_2H_2(PO_4)_{14}$	1.29
Hydroxyapatite (HA)	$Ca_{10}(PO_4)_6(OH)_2$	1.67
Carbonated hydroxyapatite (CHA)	$Ca_{10-p}(PO_4)_{6-p}(OH)_{2-p}(CO_3)_p$ $(0<p<1)$	> 1.67
Calcium-deficient HA	$Ca_{10-x}(HPO_4)_x(PO_4)_{6-x}(OH)_{2-x}$ $(0<x<1)$	1.3 – 1.67

Stoichiometric apatite is given by the chemical formula $Ca_{10}(PO_4)_6(OH)_2$, with a Ca/P atomic ratio of 1.67 (16). When apatite forms, both *in vivo* and *in vitro*, some sites for the PO_4^{3-} ion can be partially substituted by CO_3^{2-} and HPO_4^{2-} ions. One substitution of CO_3^{2-} for PO_4^{3-} results in a half Ca and one P deficiencies, thus giving a Ca/P ratio higher than 1.67. On the contrary, one substitution of HPO_4^{2-} for PO_4^{3-} results only in a half Ca deficiency, to give a Ca/P ratio lower than 1.67 (16).

Table S4. Relative elemental atomic percentages measured by EDS in ELP_3 membranes incubated in 1.5 x SBF for 5 days. The spots 1-4 are shown in Figures S2C and S2D.

Spot	C (at%)	O (at%)	N (at%)	Ca (at%)	P (at%)	O/C	N/C	Ca/P	N/Ca
1	60.4	21.3	15.7	1.5	1.1	0.35	0.26	1.4	10.5
2	65.1	21.8	12.4	0.6	0.1	0.33	0.19	6	20.7
3	52.8	25.4	17.7	2.5	1.6	0.48	0.34	1.6	7.1
4	61.2	20.9	16.7	1.0	0.2	0.34	0.27	5	16.7

Table S5. Relative elemental atomic percentages measured by EDS in ELP_3 membranes incubated in 1.5 x SBF for 7 days. The spots 1-4 are shown in Figures S2E and S2F.

Spot	C (at%)	O (at%)	N (at%)	Ca (at%)	P (at%)	O/C	N/C	Ca/P	N/Ca
1	30.3	46.0	6.1	10.9	6.6	1.52	0.20	1.7	0.56
2	33.0	48.6	3.6	9.0	5.8	1.47	0.05	1.6	0.40
3	40.4	40.0	3.9	9.6	6.1	0.99	0.10	1.6	0.41
4	67.4	17.4	13.6	1.4	0.3	0.26	0.20	4.7	9.7

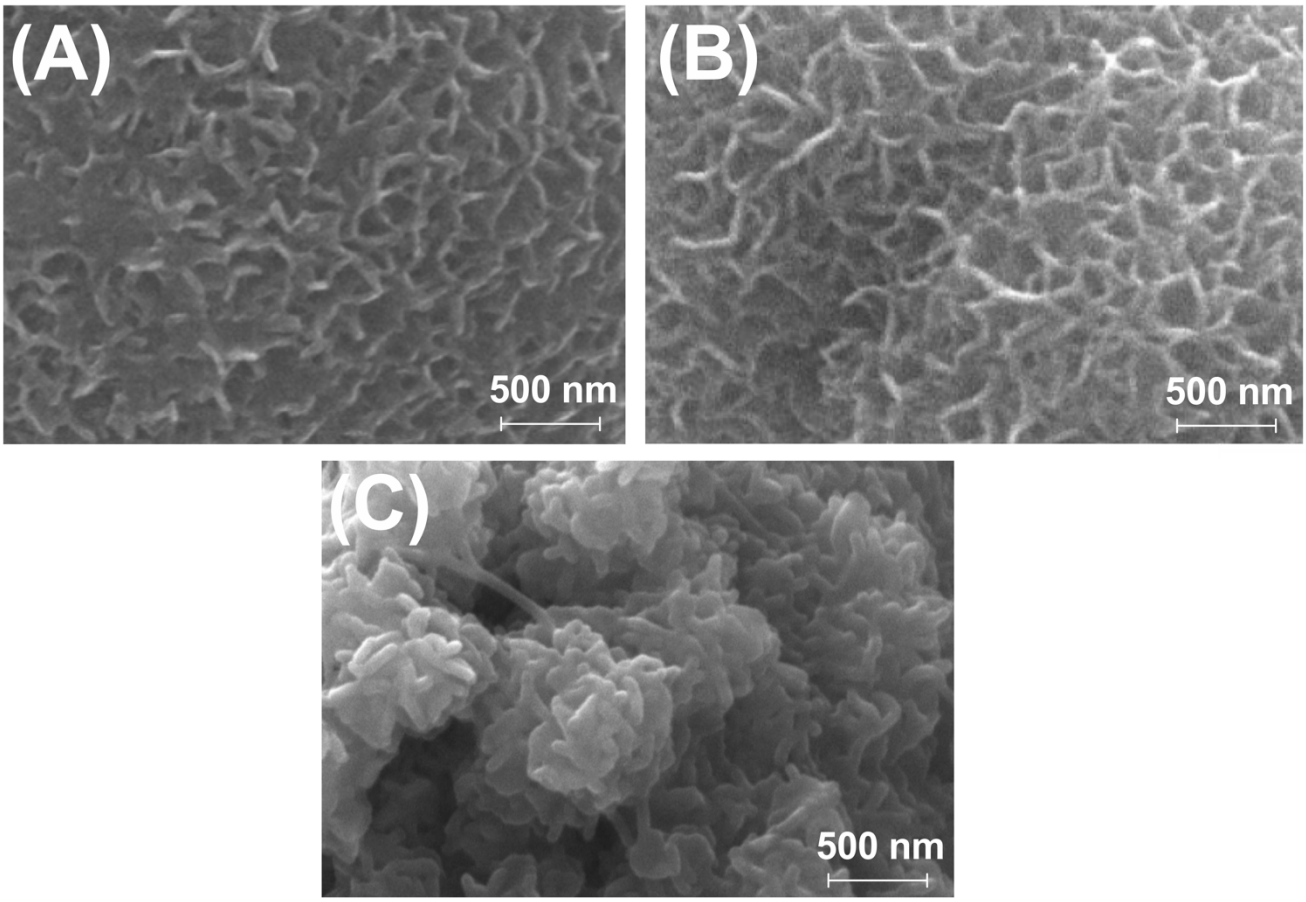

Figure S3. (**A** - **C**) Highly magnified nanoscale structures of the minerals after 7 days in (**A**) 1.5 x, (**B**) 2 x, (**C**), 3 x SBF solutions.

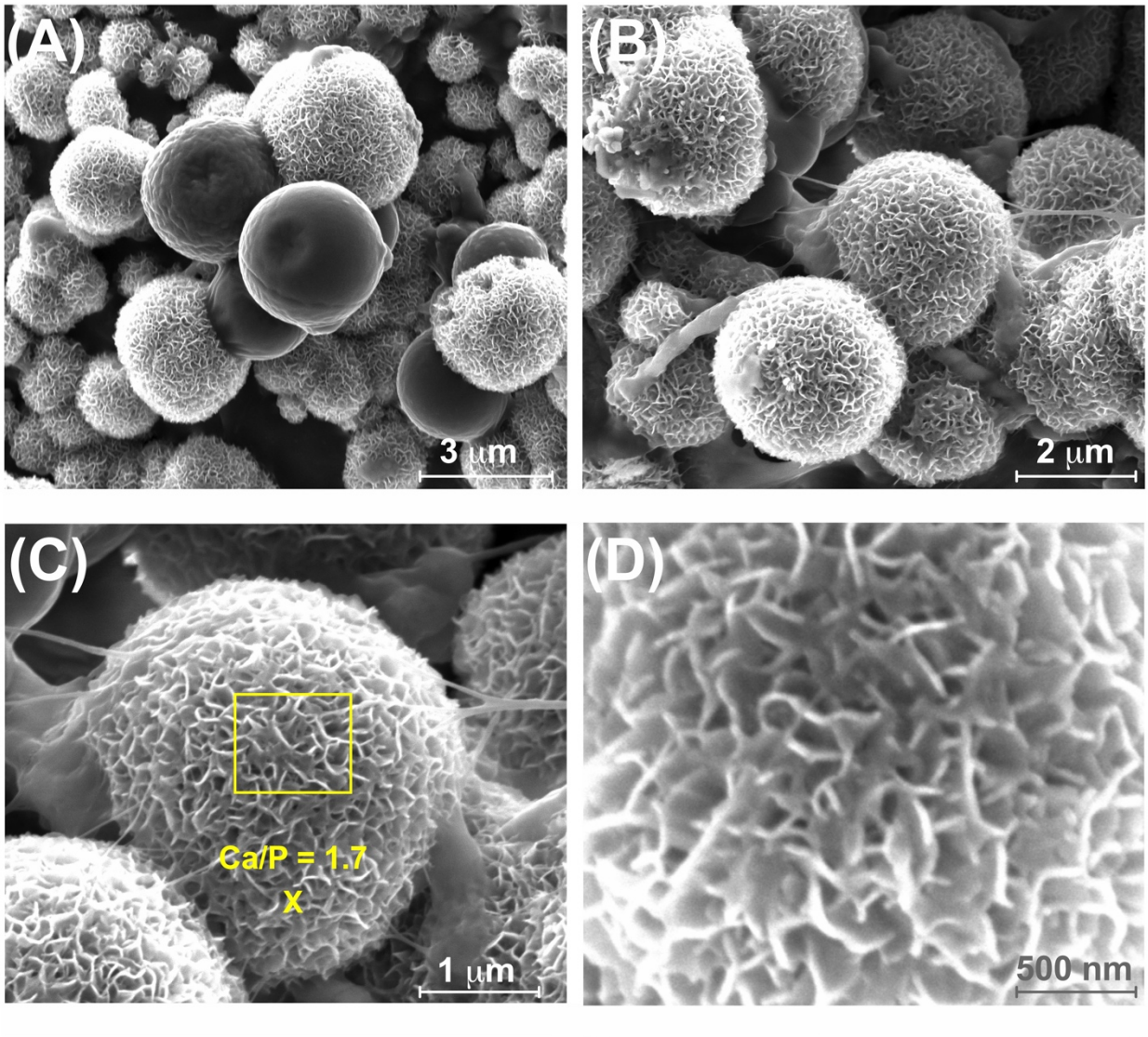

Figure S4. SEM images of ELP_3 membranes after incubation in 1.5 x SBF for 21 days. The Ca/P ratio indicated on **C** is based on elemental atomic percentages obtained by ED and (**D**) is the magnification of the highlighted region in (**C**).

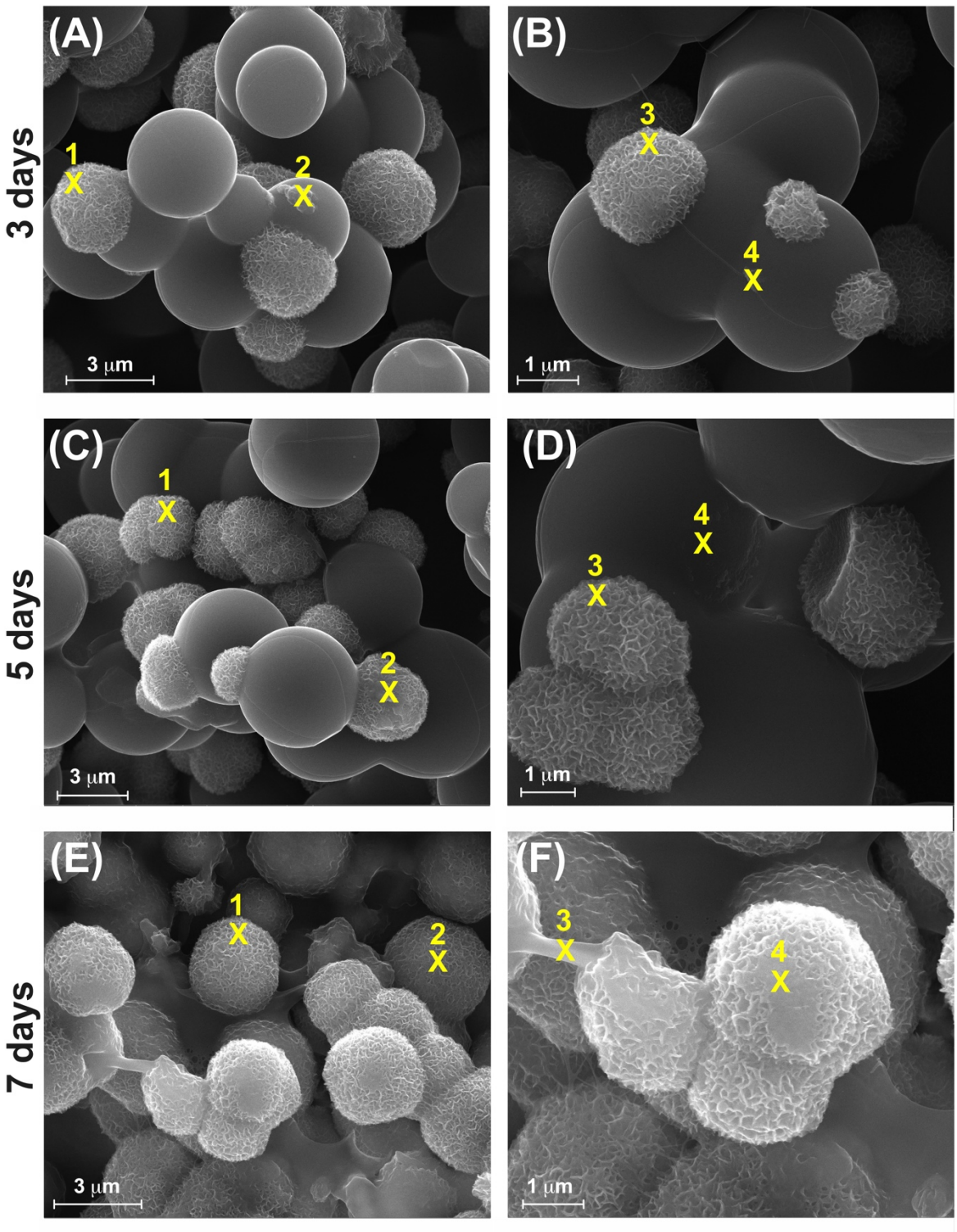

Figure S5. SEM images of ELP_3 membranes after incubation in 2 x SBF for (**A** and **B**) 3, (**C** and **D**) 5, and (**E** and **F**) 7 days. The spots marked with "X" on all panels indicate the spots where EDS spectra were collected and they correspond to the data presented in Tables S6 (spots in **A, B**), S7 (spots in **C, D**), and S8 (spots in **E, F**).

Table S6. Relative elemental atomic percentages measured by EDS in ELP_3 membranes incubated in 2 x SBF for 3 days. The spots 1-4 are shown in Figures S5A and S5B.

Spot	C (at%)	O (at%)	N (at%)	Ca (at%)	P (at%)	O/C	N/C	Ca/P	N/Ca
1	36.0	44.6	3.2	9.7	6.5	1.24	0.09	1.5	0.33
2	61.8	17.7	18.7	1.7	0.2	0.29	0.30	8.5	11.0
3	67.5	19.3	6.2	4.1	2.9	0.29	0.09	1.4	1.5
4	59.9	22.1	17.0	0.9	0.1	0.37	0.28	9.0	18.9

Table S7. Relative elemental atomic percentages measured by EDS in ELP_3 membranes incubated in 2 x SBF for 5 days. The spots 1-4 are shown in Figures S5C and S5D.

Spot	C (at%)	O (at%)	N (at%)	Ca (at%)	P (at%)	O/C	N/C	Ca/P	N/Ca
1	45.8	38.1	1.9	7.1	4.8	0.83	0.04	1.5	0.27
2	52.4	30.2	11.7	3.4	2.3	0.58	0.22	1.5	3.44
3	27.5	51.5	5.0	9.3	6.6	1.87	0.18	1.4	0.54
4	60.0	23.2	15.8	0.8	0.2	0.39	0.26	4.0	19.8

Table S8. Relative elemental atomic percentages measured by EDS in ELP_3 membranes incubated in 2 x SBF for 7 days. The spots 1-4 are shown in Figures S5E and S5F.

Spot	C (at%)	O (at%)	N (at%)	Ca (at%)	P (at%)	O/C	N/C	Ca/P	N/Ca
1	22.9	56.1	3.2	10.7	7.1	2.45	0.14	1.5	0.31
2	38.3	41.0	2.1	11.4	7.3	1.07	0.05	1.6	0.18
3	20.4	50.7	1.2	17.1	10.6	2.48	0.06	1.6	0.07
4	25.6	52.0	2.7	11.4	8.3	2.03	0.11	1.4	0.24

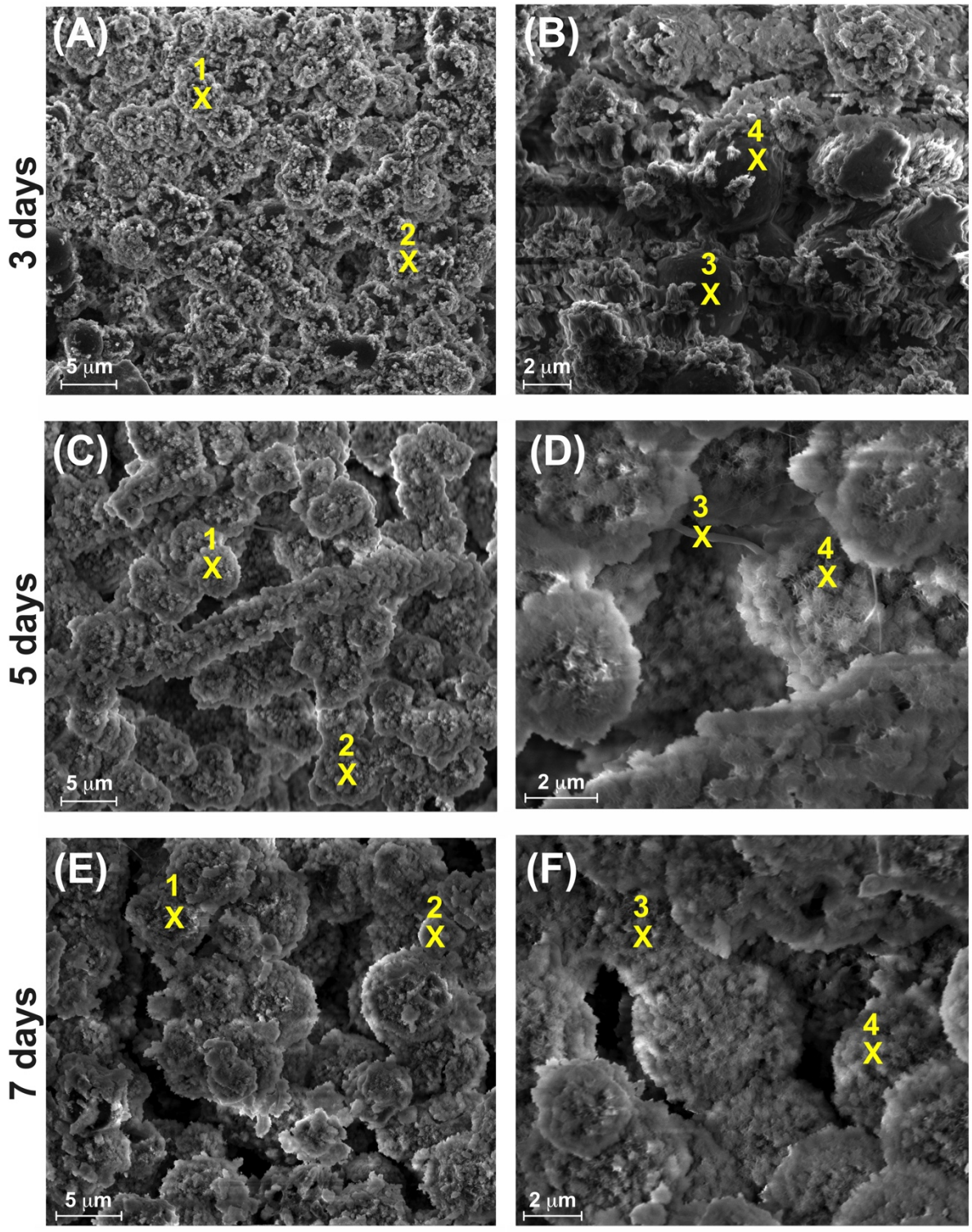

Figure S6. SEM images of ELP_3 membranes after incubation in 3 x SBF for (**A** and **B**) 3, (**C** and **D**) 5, and (**E** and **F**) 7 days. The spots marked with "X" on all panels indicate the spots where EDS spectra were collected and they correspond to the data presented in Tables S9 (spots in **A, B**), S10 (spots in **C, D**), and S11 (spots in **E, F**).

Table S9. Relative elemental atomic percentages measured by EDS in ELP_3 membranes incubated in 3 x SBF for 3 days. The spots 1-4 are shown in Figures S6A and S6B.

Spot	C (at%)	O (at%)	N (at%)	Ca (at%)	P (at%)	O/C	N/C	Ca/P	N/Ca
1	21.4	57.6	1.8	10.7	8.3	2.69	0.08	1.3	0.17
2	35.7	45.0	1.2	8.2	5.9	1.26	0.03	1.4	0.15
3	51.9	28.8	6.0	11.4	1.8	2.69	0.12	6.3	0.52
4	48.8	33.4	2.2	15.7	0.1	0.68	0.05	157	0.14

Table S10. Relative elemental atomic percentages measured by EDS in ELP_3 membranes incubated in 3 x SBF for 5 days. The spots 1-4 are shown in Figures S6C and S6D.

Spot	C (at%)	O (at%)	N (at%)	Ca (at%)	P (at%)	O/C	N/C	Ca/P	N/Ca
1	13.4	59.5	2.9	13.3	10.0	4.44	0.22	1.3	0.22
2	17.2	55.7	3.2	13.3	10.6	3.24	0.19	1.3	0.24
3	11.5	38.4	2.2	30.6	17.3	3.34	0.19	1.8	0.07
4	15.5	57.0	4.7	13.7	9.1	3.68	0.30	1.5	0.34

Table S11. Relative elemental atomic percentages measured by EDS in ELP_3 membranes incubated in 3 x SBF for 7 days. The spots 1-4 are shown in Figures S6E and S6F.

Spot	C (at%)	O (at%)	N (at%)	Ca (at%)	P (at%)	O/C	N/C	Ca/P	N/Ca
1	18.4	43.0	3.1	21.3	14.2	2.34	0.17	1.5	0.15
2	6.4	44.7	0.7	29.1	19.2	6.98	0.11	1.5	0.02
3	15.9	55.2	1.4	16.6	11.0	3.47	0.09	1.5	0.08
4	17.8	46.8	2.5	20.1	12.9	2.63	0.14	1.6	0.12

Table S12. Relative atomic percent of C, O, N, Ca, and P, and Ca/P and N/Ca ratios on ELP_3 membranes after incubation in 1.5 x, 2 x, and 3 x SBF, measured by XPS survey. No other elements were detected.

SBF solution	Time point (days)	C (at%)	O (at%)	N (at%)	Ca (at%)	P (at%)	Ca/P	N/Ca
/	0	68 ± 3	19 ± 3	13 ± 1	N	N	/	/
1.5 x SBF	3	67 ± 2	22 ± 3	11 ± 1	0.3 ± 0.1*** $^{+++}$	0.2 ± 0.1	1.5 ± 0.2	37 ± 8
	5	67 ± 1	21 ± 2	11 ± 1	0.7 ± 0.1*** $^{+++}$	0.5 ± 0.1	1.5 ± 0.1	17 ± 3
	7	66 ± 4	21 ± 2	11 ± 2	1.6 ± 0.2*** $^{+++}$	0.9 ± 0.2	1.7 ± 0.1	7 ± 2
	21	59 ± 3	23 ± 3	10 ± 1	4.8 ± 0.8	3.0 ± 0.9	1.8 ± 0.3	2.2 ± 0.6
2 x SBF	3	65 ± 2	20 ± 3	9 ± 2	3 ± 0.7***	2.1 ± 0.4	1.4 ± 0.1	3.0 ± 1.0
	5	52 ± 4	30 ± 2	8 ± 2	5.8 ± 0.8*** †	3.9 ± 0.7	1.5 ± 0.1	1.4 ± 0.6
	7	30 ± 3	49 ± 2	5 ± 1	9.8 ± 0.6*** †	6.4 ± 0.5	1.5 ± 0.1	0.6 ± 0.2
3 x SBF	3	55 ± 5	30 ± 4	8 ± 2	4.2 ± 0.9^{+++}	2.8 ± 0.8	1.5 ± 0.1	1.9 ± 0.7
	5	24 ± 3	47 ± 2	1.7 ± 0.5	15.4 ± 0.8^{+++} †	10.6 ± 0.7	1.5 ± 0.2	0.1 ± 0
	7	22 ± 3	46 ± 3	1.5 ± 0.5	18 ± 1^{+++} †	11.8 ± 0.6	1.5 ± 0.2	0.1 ± 0

* indicates significant differences between samples incubated in 1.5 x and 2 x SBF with * = P<0.02, ** = P<0.001, *** = P<0.0005.
$^{+}$ indicates significant difference between samples incubated in 1.5 x and 3 x SBF with $^{++}$ = P< 0.005, $^{+++}$ = P< 0.0001.
† indicates significant differences between samples incubated in 2 x and 3 x SBF with †† = P< 0.005, and ††† = P< 0.0001.
Three samples per condition were analyzed.

Table S13. FTIR peak assignments for calcified ELP_3 membranes and HA.

Peak (cm^{-1})	Calcified ELP_3 membrane	HA	References
v OH	3290-3300	3300	
v N-H	2958-2964		
v_{as} CH_2	2926-2929		
v_s CH_2	2865-2868		
v C=O (amide I)	1638-1642		(17), (18), (19)
v C-N, δ N-H (amide II)	1535-1540		(17), (18), (19)
δ CH_2	1443-1451		(20)
δ CH_3	1365-1372		(17), (19), (20)
δ C-H (amide III)	1232-1236		(17)
v_3 PO_4^{3-}	1109-1110	1091	(18), (21), (22), (23)
v_3 PO_4^{3-}	1027-1031	1031	(18), (21), (22), (23)
v_1 PO_4^{3-}	960-963	962	(18), (21), (22), (23)
v_2 CO_3^{2-}	864-867		(18), (21), (22), (24)
v_4 PO_4^{3-}	600-602	602	
v_4 PO_4^{3-}	561-563	564	

v_{as}: antisymmetric stretching; ν_s: symmetric stretching; δ: bending

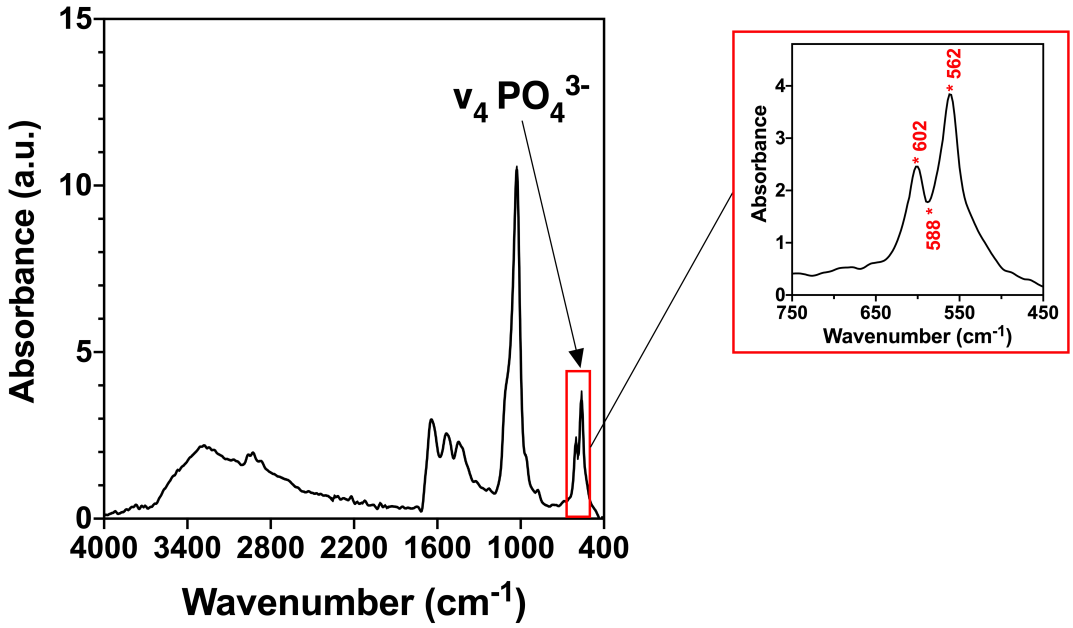

Figure S7. Representative FTIR spectrum of calcified ELP3 membraned incubated in 1.5 x SBF for 21 days showing the degenerated v_4 phosphate band used in Shemesh's method to determine the mineral crystallinity (4).

Table S14. Experimental mineral crystallinity indexes (CI) measured in calcified ELP_3 membranes and HA based on the FTIR ν_4 vibration peaks.

SBF solution	Time point (days)	CI
1.5 x SBF	7	3.3 ± 0.1* + ##
	21	4.2 ± 0.2 ##
2 x SBF	7	2.6 ± 0.2*
3 x SBF	7	2.6 ± 0.1+
HA	/	5.6 ± 0.3

* indicates significant differences between samples incubated in 1.5 x and 2 x SBF for 7 days with P<0.05.
+ indicates significant difference between samples incubated in 1.5 x and 3 x SBF for 7 days with P< 0.05.
indicates significant differences between samples incubated in 1.5 x SBF for 7 and 21 days with P< 0.02.
Three samples per condition were analyzed.

Table S15. Experimental XRD FWHM values of the peak corresponding to the planes (211), (121), and (202) in ELP_3 membranes incubated in 1.5 x SBF for 7 and 21 days, and in 2 x SBF and 3 x SBF for 7 days.

SBF solution	Time point (days)	XRD FWHM
1.5 x SBF	7	1.2 ± 0.1* $^{+}$ #
	21	0.7 ± 0.2#
2 x SBF	7	1.8 ± 0.2*
3 x SBF	7	1.9 ± 0.2^{+}

* indicates significant differences between samples incubated in 1.5 x and 2 x SBF for 7 days with P<0.05.
$^{++}$ indicates significant difference between samples incubated in 1.5 x and 3 x SBF for 7 days with P< 0.05.
# indicates significant differences between samples incubated in 1.5 x SBF for 7 and 21 days with P< 0.05.
Three samples per condition were analyzed.

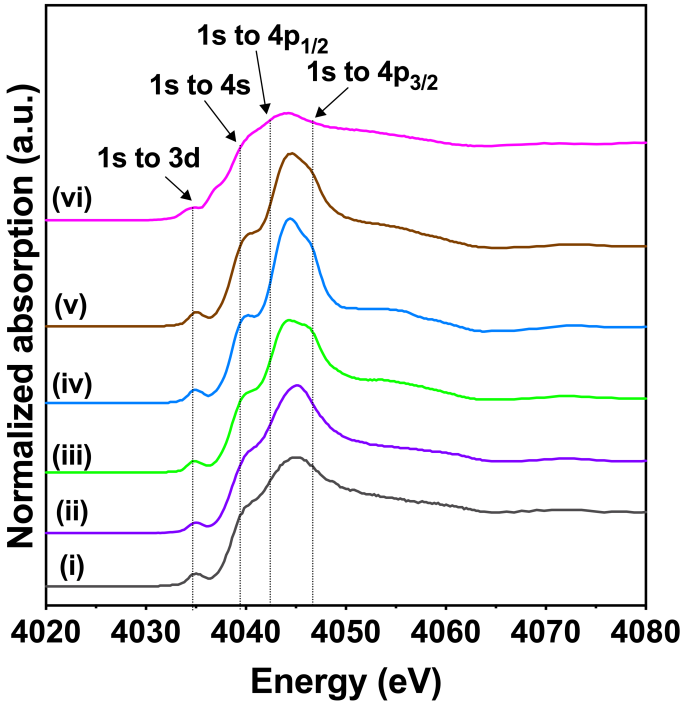

Figure S8. Representative Ca K-edge NEXAFS reference spectra of (i) ELP_3-Ca^{2+}, (ii) ACP, (iii) DCPD, (iv) OCP, (v) HA, (vi) CHA, and (vii) β-TCMP.

Table S16. Percentages of ELP_3-Ca^{2+}, ACP, OCP, HA, and CHA in ELP_3 membranes incubated in 1.5 x, 2 x, and 3 x SBF solutions determined by LCF using Ca K-edge NEXAFS spectra of reference samples, and R-factors of the LCF.

SBF solution	Time point (days)	ELP_3-Ca^{2+} (%)	ACP (%)	OCP (%)	HA (%)	CHA (%)	R-factor
1.5 x SBF	3	30 ± 5	27 ± 7$^{*\,++}$	21 ± 5^{++}	15 ± 5$^{**\,++}$	7 ± 2	0.007 ± 0.003
	5	24 ± 4^{+++}	19 ± 3$^{**\,++}$	20 ± 6^{++}	19 ± 3$^{**\,+++}$	10 ± 4	0.003 ± 0.001
	7	20 ± 4^{***+++}	16 ± 3$^{***\,+++}$	17 ± 3$^{*\,+++}$	33 ± 3$^{**\,+++}$	14 ± 5*	0.005 ± 0.002
	21	0	10 ± 3	10 ± 2	51 ± 6	29 ± 2	0.0003 ± 0.0001
2 x SBF	3	26 ± 4	11 ± 2*	14 ± 3	39 ± 6**	10 ± 4	0.005 ± 0.0002
	5	20 ± 4†††	9 ± 3**	14 ± 4	42 ± 5$^{**\,\dagger\dagger}$	15 ± 3	0.0002 ± 0.0001
	7	0***	0***	7 ± 3$^{*\,\dagger}$	68 ± 5$^{**\,\dagger}$	25 ± 5*	0.003 ± 0.001
3 x SBF	3	25 ± 4	9 ± 3^{++}	10 ± 5^{++}	46 ± 3^{++}	10 ± 4	0.002 ± 0.0005
	5	0$^{+++\,\dagger\dagger\dagger}$	4 ± 1^{++}	7 ± 3^{++}	75 ± 4$^{+++\,\dagger\dagger}$	14 ± 3	0.0004 ± 0.0001
	7	0^{+++}	0^{+++}	0†	84 ± 6†	16 ± 5	0.0004 ± 0.0001

* indicates significant differences between samples incubated in 1.5 x and 2 x SBF with * = P<0.05, ** = P<0.005, ***=P<0.0001.
$^{+}$ indicates significant difference between samples incubated in 1.5 x and 3 x SBF with $^{++}$ = P< 0.005, $^{+++}$ = P< 0.0001.
† indicates significant differences between samples incubated in 2 x and 3 x SBF with † = P< 0.05, †† = P< 0.005, and ††† = P< 0.0001.
Three samples per condition were analyzed.

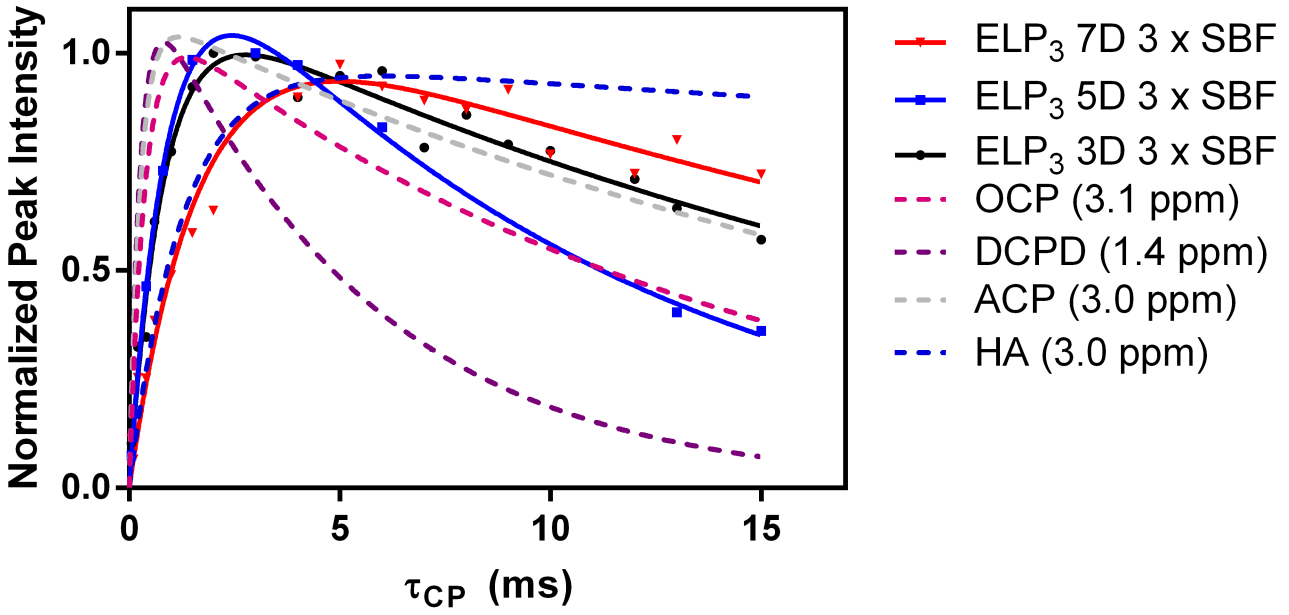

Figure S9. Integrated ^{31}P peak intensities are plotted as a function of ^{1}H-^{31}P CP contact time (τ_{CP}), for ELP_3 membranes incubated in 3 x SBF and for Ca-P standard compounds. Lines represent the best fits obtained for each data set using Eq. 1, and were used to calculate the parameters T_{CP} and T^{1}_{ρ}, shown in Table 1.

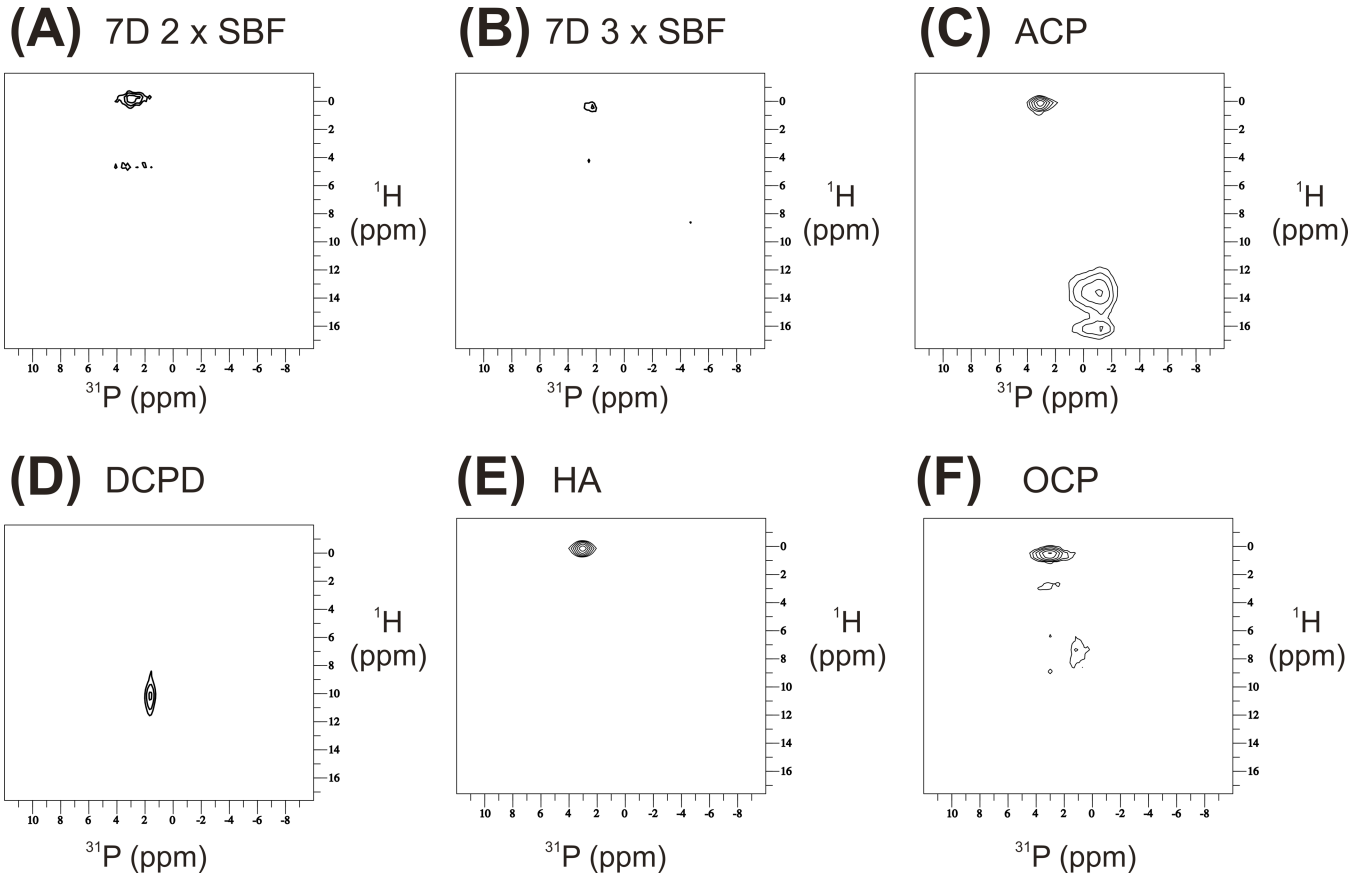

Figure S10. ^{1}H-^{31}P HETCOR spectra recorded at 10 kHz MAS for ELP_3 membranes and Ca-P reference compounds. 2D spectra are shown for samples incubated in (**A**) 2 x SBF for 7 days, (**B**) 3 x SBF for 7 days, as well as for ACP (**C**), DCPD (**D**), HA (**E**), and OCP (**F**). Each spectrum is plotted at approximately the same level above the noise, such that variations in peak intensity are representative of the signal to noise ratios in each sample.

Section 3: Supplemental references

1. Ohtsuki, C.; Kokubo, T.; Yamamuro, T., Mechanism of apatite formation on CaO-SiO2-P2O5 glasses in a simulated body fluid. *J. Noncryst. Solids.* **1992,** *143*, 84–92.
2. Davies, J., Ion association. *London: Butterworth Press.* **1962.**
3. McDowell, H.; Gregory, T. M.; Brown, W. E., Solubility of Ca5(PO4)3OH in the System Ca(OH)2–H3PO4–H2O at 5, 15, 25, and 37°C. *J. Res. Natl. Bur. Stand.* **1977,** *81A*, 273– 281.
4. Shemesh, A., Crystallinity and diagenesis of sedimentary apatites. *Geochim. Cosmochim. Acta.* **1990,** *54* (9), 2433-2438.
5. Termine, J.; Posner, A., Infrared analysis of rat bone: Age dependency of amorphous and crystalline mineral fraction. *Science.* **1966,** *113* (3743), 1523-1525.
6. Koningsberger, D.; Mojet, B.; Van Dorssen, G.; Ramaker, D., XAFS spectroscopy; fundamental principles and data analysis. *Top. Catal.* **2000,** *10* (3-4), 143–155.
7. Gourgas, O.; Marulanda, J.; Zhang, P.; Murshed, M.; Cerruti, M., Multidisciplinary Approach to Understand Medial Arterial Calcification. *Arterioscler. Thromb. Vasc. Biol.* **2018,** *38* (2), 363-372.
8. LeGeros, R., Formation and transformation of calcium phosphates: relevance to vascular calcification. *Z. Kardiol.* **2001,** *90* (3), 116-124.
9. Schlieper, G.; Aretz, A.; Verberckmoes, S.; Krüger, T.; Behets, G.; Ghadimi, R.; Weirich, T.; Rohrmann, D.; Langer, S.; Tordoir, J.; Amann, K.; Westenfeld, R.; Brandenburg, V.; D'Haese, P.; Mayer, J.; Ketteler, M.; McKee, M.; Floege, J., Ultrastructural analysis of vascular calcifications in uremia. *J. Am. Soc. Nephrol.* **2010,** *21* (4), 689–696.
10. Verberckmoes, S.; Persy, V.; Behets, G.; Neven, E.; Hufkens, A.; Zebger-Gong, H.; Müller, D.; Haffner, D.; Querfeld, U.; Bohic, S.; De Broe, M.; D'Haese, P., Uremia-related vascular calcification: more than apatite deposition. *Kidney Int.* **2007,** *71* (4), 298–303.
11. Cottignoli, V.; Cavarretta, E.; Salvador, L.; Valfré, C.; Maras, A., Morphological and chemical study of pathological deposits in human aortic and mitral valve stenosis: a biomineralogical contribution. *Patholog. Res. Int.* **2014,** *2015*, 1-14.
12. Prieto, R.; Gomila, I.; Söhnel, O.; Costa-Bauza, A.; Bonnin, O.; Grases, F., Study on the structure and composition of aortic valve calcific deposits: etiological aspects. *J. Biophys. Chem.* **2011,** *2* (1), 19–25.
13. Gourgas, O.; Muiznieks, L.; Guadarrama Bello, D.; Nanci, A.; Sharpe, S., Crosslinked Elastin-Like Polypeptide Membranes as a Model for Medial Arterial Calcification. *Biomacromolecules* **2019,** *20* (7), 2625-2636.
14. Gaur, A.; Shrivastava, B.; Joshi, S., Copper K-edge XANES of Cu (I) and Cu (II) oxide mixtures. *J. Phys.: Conf. Ser.* **2009,** *190*, 012084.
15. Ravel, B.; Newville, M., ATHENA, ARTEMIS, HEPHAESTUS: data analysis for X-ray absorption spectroscopy using IFEFFIT. *J. Synchrotron Radiat.* **2005,** *12* (pt4), 537–541.
16. Cosmidis, J.; Benzerara, K.; Nassif, N.; Tyliszczak, T.; Bourdelle, F., Characterization of Ca-phosphate biological materials by scanning transmission X-ray microscopy (STXM) at the Ca L2,3-, P L2,3- and C K-edges. *Acta Biomater.* **2015,** *12*, 260–269.
17. Popescu, M.; Vasile, C.; Craciunescu, O., Structural analysis of some soluble elastins by means of FT-IR and 2D IR correlation spectroscopy. *Biopolymers.* **2010,** *93* (12), 1072-1084.
18. Vyavahare, N.; Ogle, M.; Schoen, F.; Levy, R., Elastin Calcification and its Prevention with Aluminum Chloride Pretreatment. *Am. J. Pathol.* **1999,** *155* (3), 973–982.
19. Serrano, V.; Liu, W.; Franzen, S., An Infrared Spectroscopic Study of the Conformational Transition of Elastin-Like Polypeptides. *Biophys. J.* **2007,** *93* (7), 2429–2435. .

20. Belbachir, K.; Noreen, R.; Gouspillou, G.; Petibois, C., Collagen types analysis and differentiation by FTIR spectroscopy. *Anal. Bioanal. Chem.* **2009,** *395* (3), 829-837.
21. Salenius, J.; Brennan, J.; Miller, A.; Wang, Y.; Aretz, T.; Sacks, B.; Dasari, R.; Feld, M., Biochemical composition of human peripheral arteries examined with Near-Infrared Raman Spectroscopy. *J. Vasc. Surg.* **1998,** *27* (4), 710-719.
22. Koutsopoulos, S., Synthesis and Characterization of hydroxyapatite crystals: a review study on the analytical methods. *J. Biomed. Mater. Res., Part A* **2002,** *62* (4), 600-612.
23. Rey, C.; Shimizu, M.; Collins, B.; Glimcher, M. J., Resolution-enhanced Fourier transform infrared spectroscopy study of the environment of phosphate ions in the early deposits of a solid phase of calcium-phosphate in bone and enamel, and their evolution with age. I: Investigations in the v4 PO4 domain. *Calcif. Tissue Int.* **1990,** *46*, 384-394.
24. Rey, C.; Renugopalakrishnan, V.; Shimizu, M.; Collins, B.; Glimcher, M. J., A resolution-enhanced Fourier Transform Infrared spectroscopic study of the environment of the CO32− ion in the mineral phase of enamel during its formation and maturation. *Calcif. Tissue Int.* **1991,** *49* (4), 259–268.